



Short communication

# 1,2,3,4-Tetrahydroisoquinoline/2H-chromen-2-one conjugates as nanomolar P-glycoprotein inhibitors: Molecular determinants for affinity and selectivity over multidrug resistance associated protein 1

Mariagrazia Rullo, Mauro Niso, Leonardo Pisani\*, Antonio Carrieri, Nicola Antonio Colabufo, Saverio Cellamare, Cosimo Damiano Altomare

Dipartimento di Farmacia-Scienze Del Farmaco, Università Degli Studi di Bari "Aldo Moro", via E. Orabona 4, 70125, Bari, Italy

## ARTICLE INFO

## Article history:

Received 11 August 2018

Received in revised form 15 October 2018

Accepted 16 October 2018

Available online xxx

## Keywords:

Multidrug resistance

Coumarin

Structure-activity relationships

P-glycoprotein

Multidrug resistance associated protein 1

Molecular docking

## ABSTRACT

A series of conjugates bearing a 1,2,3,4-tetrahydroisoquinoline motif linked to substituted 7-hydroxy-2H-chromen-2-ones was synthesized and assayed through calcein-AM test in Madin-Darby Canine Kidney (MDCK) cells overexpressing P-glycoprotein (P-gp) and closely related multidrug resistance associated protein 1 (MRP1) to probe the interference with efflux mechanisms mediated by P-gp and MRP1, respectively. A number of substituents at C3 and C4 of coumarin nucleus along with differently sized and shaped spacers was enrolled to investigate the effects of focused structural modifications over affinity and selectivity. Linker length and flexibility played a key role in enhancing P-gp affinity as proved by the most potent P-gp modulator (**3h**,  $IC_{50}=70$  nM). A phenyl ring within the spacer (**3k**, **3l**, **3o**) and bulkier groups (Br in **3r**, Ph in **3u**) at coumarin C3 led to derivatives showing nanomolar activity ( $160$  nM  $< IC_{50} < 280$  nM) along with outstanding selectivity over MRP1 ( $SI > 350$ ). Molecular docking calculations carried out on a human MDR1 homology model structure contributed to gain insight into the ligands' binding modes. Some compounds (**3d**, **3h**, **3l**, **3r**, **3t**, **3u**) reversed MDR thereby restoring doxorubicin cytotoxicity when co-administered with the drug into MDCK-MDR1 cells.

© 2018.

## Abbreviations

ABC	ATP-binding cassette
AD	Alzheimer's disease
BBB	blood-brain barrier
Calcein-AM	calcein acetoxymethyl ester
CYP450 3A	cytochrome P450 3A
DIPEA	diisopropylethylamine
DMEM	Dulbecco's modified Eagle's medium
DMSO	dimethyl sulfoxide
DNA	deoxyribonucleic acid
FBS	fetal bovine serum
FEB	free energy of binding
LE	ligand efficiency
LLE	lipophilic ligand efficiency
MDCK	Madin-Darby Canine Kidney
MDR	multidrug resistance
MDR1	multidrug resistance protein 1
MRP1	multidrug resistance-associated protein 1
MTT	3-(4,5-dimethylthiazol-2-yl)-2,5-diphenyltetrazolium bromide

MW	microwave
NBS	N-bromosuccinimide
PBS	phosphate buffered saline
PD	Parkinson's disease
PEG	polyethylene glycol
P-gp	P-glycoprotein
SEM	standard error mean
SI	selectivity index
THIQ	1,2,3,4-tetrahydroisoquinoline)

## 1. Introduction

Cancer cells may become unresponsive to chemotherapeutics through a phenomenon termed multidrug-resistance (MDR) affecting agents structurally and mechanistically unrelated [1]. Both genetic and epigenetic alterations can modulate drug sensitivity by activating different mechanisms [2]: i) reduced drug uptake; ii) up-regulation of defensive machineries (DNA repair and/or cytochrome P450 mixed-function oxidases); iii) interruption of apoptosis signalling. In addition, a major role is featured by the overexpression of energy-dependent ATP-binding cassette (ABC) transporter proteins [3], that detoxify cancer cells and lower intracellular concentration under the therapeutic threshold by pumping drugs out at the expense of ATP hydrolysis. The human ABC superfamily counts 48 efflux pumps that are expressed at basal levels in normal tissues where serve cells as shut-

\* Corresponding author.

Email address: leonardo.pisani@uniba.it (L. Pisani)

tles for a variety of xenobiotics and endogenous substances (e.g., lipids, peptides, and ions) [4]. Several members have been clearly associated with MDR, including P-glycoprotein (P-gp, also called multidrug resistance protein 1, MDR1, or ABCB1) and multidrug resistance-associated protein 1 (alternatively termed MRP1 or ABCC1) (see Chart 1).

P-gp is by far the most studied protein [5], that has been found in epithelial cells membranes of different districts, such as kidney and liver. Furthermore, P-gp protects brain by extruding toxins into blood at the luminal interface of blood-brain barrier (BBB). MRP1 is ubiquitously expressed and transports preferentially anionic substrates and glutathione conjugates [6]. Both P-gp and MRP1 are widely expressed in many leukaemias and solid tumors.

The inhibition of ABC pumps, especially P-gp, has long been considered a viable target to circumvent resistance and ameliorate the clinical outcome of chemotherapeutic agents. Unfortunately, tested MDR reversers did not score relevant efficacy in clinical trials because of impeding challenges represented by toxicity/selectivity issues and pharmacokinetic interactions arising from CYP450 3A inhibition. Therefore, alternative strategies to evade MDR have been envisaged through innovative drug delivery approaches that bypass ABC proteins inhibition [7]. However, small molecule P-gp binders are still needed to better understand molecular recognition interactions and provide safer tools to co-adjuvate chemotherapy [8]. Moreover, P-gp overexpression at the BBB level has been observed in the early stage of neurodegenerative syndromes such as Alzheimer's disease (AD) and Parkinson's disease (PD) and some ligands are under evaluation as imaging tracers [9].

With the aim of gaining further knowledge about P-gp binding interactions and exploring molecular determinants for selectivity over another ABC pump (e.g., MRP1), herein we report the design, synthesis and biological evaluation of novel conjugates where a 1,2,3,4-tetrahydroisoquinoline (THIQ) moiety was linked to a 7-hydroxy-2H-chromen-2-one (coumarin) scaffold through differently shaped and sized spacers. On one hand, the protonatable THIQ nucleus is recurrent in several selective P-gp inhibitors (e.g., tariquidar) as well as non-selective compounds (e.g., elacridar). On the other hand,

coumarin motif is a nature-friendly, easy-to-handle chemical building block that has been exploited in several medicinal chemistry programs (e.g., addressing cancer [10] and neurodegeneration [11,12]) and in few studies focused on P-gp ligands bearing lamellarin-type alkaloid skeleton [13]. Polymethylene and *ortho*-, *meta*-, *para*-xylyl chains were explored as the spacers connecting the two heterocyclic cores. Moreover, the effect of methyl groups, halogens (Cl, Br), and phenyl rings at position 3 and 4 of the coumarin was investigated, as well as few modifications on the basic moiety regarding the presence of 6,7-dimethoxy substitution. All the title compounds were tested in the calcein-AM (calcein acetoxymethyl ester) uptake assay across MDCK-MDR1 and MDCK-MRP1 cells to evaluate the interference with the pro-fluorescent substrate transport by MDR1 and MRP1 pumps, respectively. The binding contacts within P-gp framework were investigated by means of computer-aided molecular docking simulations. Moreover, cell-based co-incubation experiments with a well-known anticancer drug (doxorubicin) were supplied to probe the MDR reverting skills for a number of highly potent P-gp inhibitors.

## 2. Methods

### 2.1. Chemistry

The synthetic route for the preparation of novel compounds **3a-v** is shown in Scheme 1. Starting 7-hydroxycoumarins were commercially available (**1b**, **1d**) or prepared on a laboratory scale by following literature procedures with slight modifications. The well-known von Pechmann condensation was employed to synthesize 7-hydroxy-3,4-dimethyl-2H-chromen-2-one [14] (**1a**) and 7-hydroxy-4-methyl-2H-chromen-2-one [15], whose regioselective NBS-mediated aromatic bromination [16] in PEG-400 furnished **1c**. Cyclo-condensation of the suitable 2-hydroxyacetophenone or salicylaldehyde with phenacetylchloride or phenylacetic acid, respectively, furnished 3-phenylcoumarins **1e-f** [17,18]. Methyl-ether cleavage promoted by a Lewis acid (AlCl<sub>3</sub>) provided **1g** from 3-methoxy-6H-benzo[*c*]chromen-6-one [15]. A microwave-assisted nucleophilic substitution between the appropriate hydroxycoumarin

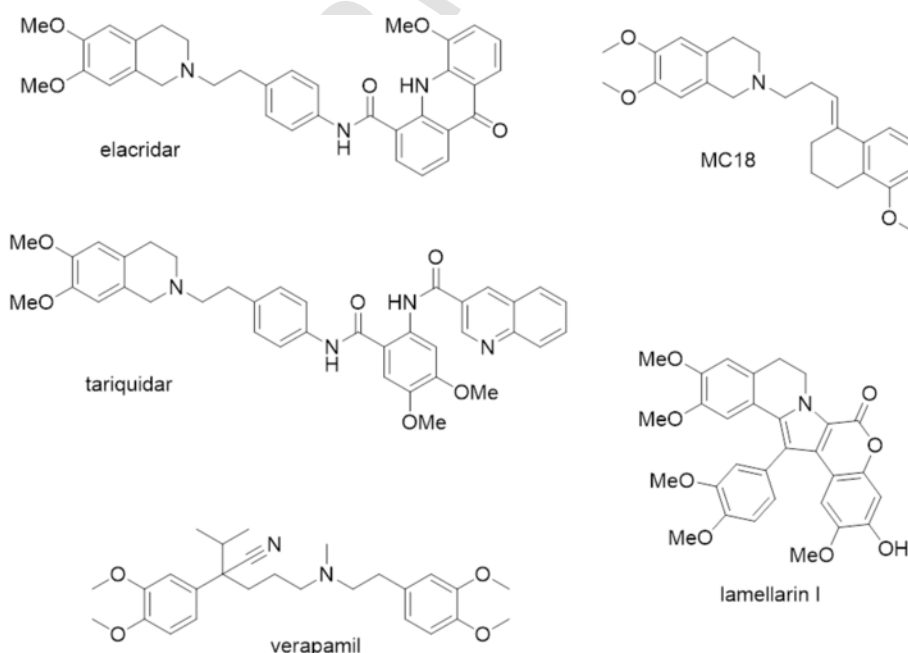
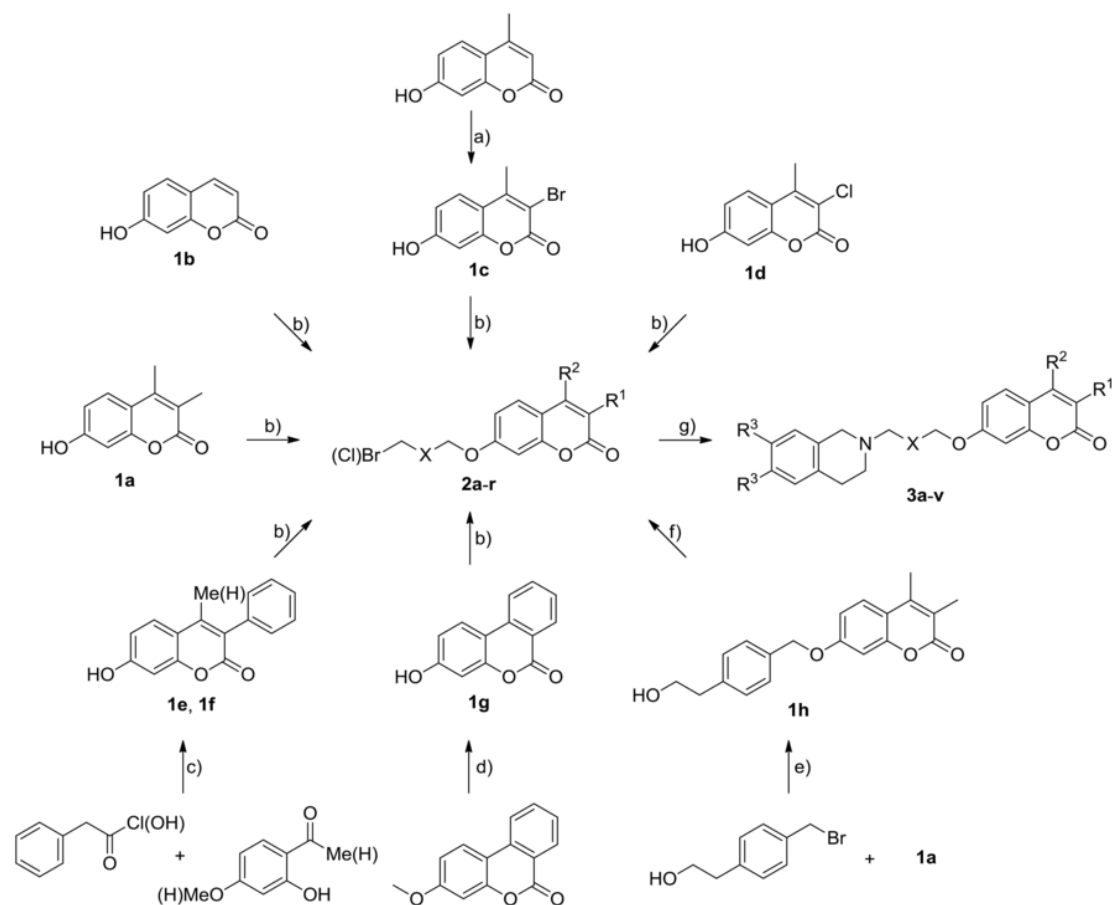


Chart 1. Chemical structures of known P-gp ligands.



**Scheme 1.** Synthesis of compounds **3a-v**. <sup>a</sup> Reagents and conditions: a) *N*-bromosuccinimide, PEG-400, room temperature, 3 h; b) for **2a-g**, **2i-r**: an.  $K_2CO_3$ , suitable di-halide ( $\alpha,\alpha'$ -dibromo(chloro)-xylenes, *trans*-1,4-dibromo-2-butene or 1, $\omega$ -dibromoalkanes), KI (cat.), anhydrous acetone, 130°C, 30 min, MW; c) for **1e** from phenylacetic acid and 2-hydroxy-4-methoxybenzaldehyde see Ref. [17]; for **1f**: 2',4'-dihydroxyacetophenone, phenylacetylchloride, an.  $K_2CO_3$ , an. acetone, reflux, 4 h; d) an.  $AlCl_3$ , *o*-xylene, reflux, 9 h; e) an.  $K_2CO_3$ , KI (cat.), anhydrous acetone, 130°C, 30 min, MW; f)  $CBR_4$ ,  $PPh_3$ , an. dichloromethane, 0°C to room temperature, 4 h; g) suitable 1,2,3,4-tetrahydroisoquinoline hydrochloride, DIPEA, KI (cat.), anhydrous acetonitrile, reflux, 1 h.

cess dihalide (1, $\omega$ -dibromoalkane or  $\alpha,\alpha'$ -dibromo(chloro)-xylene) yielded the intermediates **2a-g** and **2i-r**. In a similar way, alkylation of **1a** with 2-[4-(bromomethyl)phenyl]ethanol furnished alcohol **1h** that in turn underwent an Appel-type bromination to **2h**. The mono-halo derivatives **2a-r** were reacted with the suitable THIQ in refluxing acetonitrile in the presence of DIPEA to prepare final compounds **3a-v**.

## 2.2. Biological activity evaluation

### 2.2.1. Calcein-AM assay

Compounds **3a-v** were screened as inhibitors of P-gp and MRP1 mediated transport in the fluorescence-based Calcein-AM assay by using MDCK cell lines overexpressing MDR1 and MRP1, respectively. Data are reported in Table 1 and  $IC_{50}$  values ( $\mu M$ ) are compared with MC18 [19] and verapamil taken as reference MDR1 and MRP1 inhibitors, respectively. In order to evaluate the selectivity between the two transporters, the selectivity index (SI) was calculated as the ratio  $IC_{50} (MRP1)/IC_{50} (P-gp)$ .

### 2.2.2. Antiproliferative assay

3-(4,5-Dimethylthiazol-2-yl)-2,5-diphenyltetrazolium bromide (MTT) assay [20] was used to measure the percentage of viable MDCK-MDR1 cells after incubation with tested compounds (**3d**, **3h**, **3l**, **3r**, **3t**, **3u**) at three different concentrations (0.1, 1 and 10  $\mu M$ )

alone and in co-administration with doxorubicin (10  $\mu M$ ), in order to evaluate the capacity of compounds to circumvent resistance to the chemotherapeutic drug and to re-establish the anti-proliferative activity.

## 2.3. Computational studies

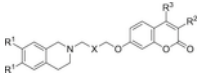
Conformational sampling in aqueous environment of the most active compound **3h** was first performed throughout molecular dynamics followed by dockings to the MDR1 binding site. The previously published human P-gp homology model [21] was chosen as biomolecular target to investigate plausible binding modes of the most potent inhibitor **3h** and to gain valuable insights into the protein sites where the two heterocyclic moieties (THIQ and coumarin) most likely settle.

## 3. Results and discussion

### 3.1. Structure-activity relationships (SARs)

Noticeably, all compounds showed submicromolar P-gp inhibition with only three exceptions (**3a**, **3b** and **3j**). Conversely, only a moderate modulation of MRP1 efflux was always observed. The presence of 6,7-dimethoxy substitution pattern at the THIQ basic moiety enhanced P-gp affinity in comparison to the unsubstituted THIQs

**Table 1**  
Biological activity of compounds 3a-v towards the inhibition of MDR1- and MRP1-mediated calcein-AM efflux.

compd			R <sup>2</sup>	R <sup>3</sup>	IC <sub>50</sub> (μM) <sup>a</sup>	SI <sup>f</sup>
	R <sup>1</sup>	X				
MC18 <sup>d</sup>					1.2±0.32	
verapamil <sup>e</sup>					1.3±0.24	4.5±0.51
<b>3a</b>	H	–	Me	Me	15±1.5	>100
<b>3b</b>	H	CH <sub>2</sub>	Me	Me	2.7±0.52	73±5.2
<b>3c</b>	H	(CH <sub>2</sub> ) <sub>2</sub>	Me	Me	0.91±0.21	40±3.3
<b>3d</b>	H	(CH <sub>2</sub> ) <sub>3</sub>	Me	Me	0.55±0.10	31±3.7
<b>3e</b>	MeO	–	Me	Me	0.38±0.081	20±1.9
<b>3f</b>	MeO	CH <sub>2</sub>	Me	Me	0.19±0.017	41±4.5
<b>3g</b>	MeO	(CH <sub>2</sub> ) <sub>2</sub>	Me	Me	0.15±0.016	33±2.8
<b>3h</b>	MeO	(CH <sub>2</sub> ) <sub>3</sub>	Me	Me	0.070±0.011	12.9±1.9
<b>3i</b>	MeO	(CH <sub>2</sub> ) <sub>4</sub>	Me	Me	0.22±0.038	44±3.7
<b>3j</b>	MeO	<i>trans</i> -CH=CH	Me	Me	1.0±0.31	18±2.1
<b>3k</b>	MeO	<i>p</i> -C <sub>6</sub> H <sub>4</sub>	Me	Me	0.19±0.027	>100
<b>3l</b>	MeO	<i>p</i> -CH <sub>2</sub> C <sub>6</sub> H <sub>4</sub>	Me	Me	0.19±0.018	>100
<b>3m</b>	MeO	<i>m</i> -C <sub>6</sub> H <sub>4</sub>	Me	Me	0.16±0.010	3.6±0.52
<b>3n</b>	MeO	<i>m</i> -C <sub>6</sub> H <sub>4</sub>	H	H	0.77±0.081	3.7±0.64
<b>3o</b>	MeO	<i>o</i> -C <sub>6</sub> H <sub>4</sub>	Me	Me	0.16±0.018	>100
<b>3p</b>	MeO	(CH <sub>2</sub> ) <sub>2</sub>	Cl	Me	0.56±0.056	53±6.5
<b>3q</b>	MeO	(CH <sub>2</sub> ) <sub>3</sub>	Cl	Me	0.46±0.037	18±0.63
<b>3r</b>	MeO	(CH <sub>2</sub> ) <sub>3</sub>	Br	Me	0.28±0.026	>100
<b>3s</b>	MeO	(CH <sub>2</sub> ) <sub>2</sub>	Ph	H	0.41±0.027	>100
<b>3t</b>	MeO	(CH <sub>2</sub> ) <sub>3</sub>	Ph	H	0.39±0.036	>100
<b>3u</b>	MeO	(CH <sub>2</sub> ) <sub>3</sub>	Ph	Me	0.22±0.029	>100
<b>3v</b>	MeO	(CH <sub>2</sub> ) <sub>3</sub>	Ph		0.33±0.047	>100

<sup>a</sup> Values are the mean±SEM of two independent experiments performed in triplicate.

<sup>b</sup> IC<sub>50</sub> determined in MDCK-MDR1 cell lines.

<sup>c</sup> IC<sub>50</sub> determined in MDCK-MRP1 cells.

<sup>d</sup> P-gp inhibition positive control.

<sup>e</sup> MRP1 inhibition positive control.

<sup>f</sup> Selectivity index (SI) calculated from the equation: IC<sub>50</sub> (MRP1)/IC<sub>50</sub> (P-gp).

(**3e**>**3a**, **3f**>**3b**, **3g**>**3c**, **3h**>**3d**). The distance between the two bicycles appeared as a critical structural determinant and the length of the alkyl spacer strongly affected the P-gp mediated efflux inhibition. Among the conjugates **3a-i** bearing a polymethylene alkyl chain, the inhibition potency progressed up to 5 units in the two series of analogues (**3a** < **3b** < **3c** < **3d** and **3e** < **3f** < **3g** < **3h**, from 2 to 5 methylene groups). The inhibition data clearly indicate that a pentamethylene linker optimized the interactions of both heterocyclic cores into hydrophobic binding pockets, which led to the most potent inhibitor of the series (**3h**) endowed with nanomolar P-gp activity (IC<sub>50</sub>=70 nM) and high selectivity over MRP1 (SI=184). Further elongation reduced the inhibitory potency (**3i**<**3h**). A more rigid geometry due to a *trans* double bond in the spacer resulted detrimental, as can be inferred from the comparison of **3j** with **3f** as well as **3g**. The introduction of a phenyl ring in the linker provided 3,4-dimethylcoumarins **3k**, **3m**, and **3o** that resulted equipotent or less active than their open-chain saturated analogue **3h**, **3g**, **3f**. This clue might rule out additional interactions (e.g., π-π stacking) involving the linker, which essentially works by placing the two heterocyclic heads in the best binding topology and/or produces different desolvation penalties. Interestingly, an outstanding selectivity increase was returned by both the most elongated (*para*, **3k**, SI>526) and the most constrained (*ortho*, **3o**, SI>625) regioisomer, that resulted inactive towards MRP1. Conversely, it is worth noting that the *meta*-isomer **3m** proved to be the most potent MRP1 inhibitor of the whole series (IC<sub>50</sub>=3.6 μM). The homologation of the bridge between the basic nitrogen and the phenyl ring of the spacer (**3l** vs. **3k**) did not affect neither P-gp affini-

ty nor selectivity over MRP1 while potentially improving solubility at physiological pH depending upon pK<sub>a</sub> modulation.

Focused modifications were also probed at the position 3 and 4 of the coumarin template where dimethyl substitution performed the best fitting into P-gp binding cavities. In fact, the removal of both methyl groups reduced P-gp inhibition (**3n**<**3m**) without affecting MRP1 transport. Moreover, the replacement of methyl at the position 3 in **3p-q** with Cl, having close van der Waals volume but opposite electronic effect, decreased the activity towards P-gp (**3p**<**3g**, **3q**<**3h**).

An interesting sensitivity to steric hindrance discriminated the two transporters upon binding compounds bearing a bulky substituent linked to coumarin C3 (**3r-u**) or fused to positions 3 and 4.

(**3v**). P-gp succeeded in accommodating both derivatives bearing a Br-atom (**3r**, IC<sub>50</sub>=0.28 μM) or a phenyl group at position 3 (**3s**, IC<sub>50</sub>=0.41 μM; **3t**, IC<sub>50</sub>=0.39 μM; **3u**, IC<sub>50</sub>=0.22 μM), and the more flat condensed congener **3v** (IC<sub>50</sub>=0.33 μM), whereas MRP1 did not tolerate these substituents and the compounds **3r-v** were ineffective in modulating its transport activity. This molecular discrimination resulted in excellent selectivities towards P-gp (for **3r-v**, 244<SI<455). Moreover, the presence at position 3 of a flag methyl, forcing out-of-the-plane phenyl rotation, improved P-gp modulation and selectivity (**3u**>**3s-t**) (see Fig. 1).

### 3.2. MDR reverting effect

Among the most active modulators, diverse active compounds (**3d**, **3h**, **3l**, **3r**, **3t**, **3u**) were assayed for their ability to revert resis-

tance to doxorubicin affecting MDCK-MDR1 cells that overexpress P-gp. As illustrated in Fig. 2, all compounds showed a dose-dependent potentiation of doxorubicin ( $10\ \mu\text{M}$ ) cytotoxicity and were able to restore the anti-proliferative effect of the chemotherapeutic on resistant cells upon inhibition of P-gp mediated drug efflux. Interestingly, the most potent inhibitor of the whole series (compound **3h**) showed a remarkable reduction of cell viability already at a concentration ( $0.1\ \mu\text{M}$ ) close to its  $\text{IC}_{50}$  value ( $0.070\ \mu\text{M}$ ). Moreover, at the highest concentration used ( $10\ \mu\text{M}$ ) all the derivatives under investigation showed no inherent cytotoxicity along with the most significant reverting activity observed (see Fig. 3).

In view of further drug-like optimization program, it is worth noting that compounds **3h** and **3r** behaved as potent reversers with improved efficiency metrics (ligand efficiency, LE, and lipophilic ligand efficiency, LLE) as detailed in Table 2 compared to tariquidar and elacridar, marketed drugs belonging to the third P-gp non-competitive inhibitors' generation.

### 3.3. Molecular docking simulations

A structure-based analysis of the ligand-P-gp interactions was carried on the most potent P-gp inhibitor **3h**, as representative of the novel molecular dataset. A previously reported human P-gp homology model [21] was used as the protein target. Docking simulations highlighted two distinct and adjacent lipophilic clefts of P-gp able to adequately accommodate the heterocyclic moieties of the inhibitor by means of hydrophobic interactions (van der Waals contacts or  $\pi$ - $\pi$  stacking). In details, the THIQ head is accommodated in a pocket lined by Tyr310, Phe336, Phe728, Phe732, Leu975, Phe983 whereas the coumarin tail is merged in a more widened cavity surrounded by Tyr953, Phe978 and Val982. In addition, the ligand-protein complex was stabilized by polar and hydrogen bonding contacts involving the hydroxyl of Tyr310, close to the methoxy groups in positions 6 and 7 of the THIQ moiety, and those occurring between the protonated nitrogen and the sulphur atom of Met69 side chain. The crucial role of the methoxy substituents as chemical fingerprint on the THIQ ring was corroborated by the lower activity of compounds **3a-d** lacking

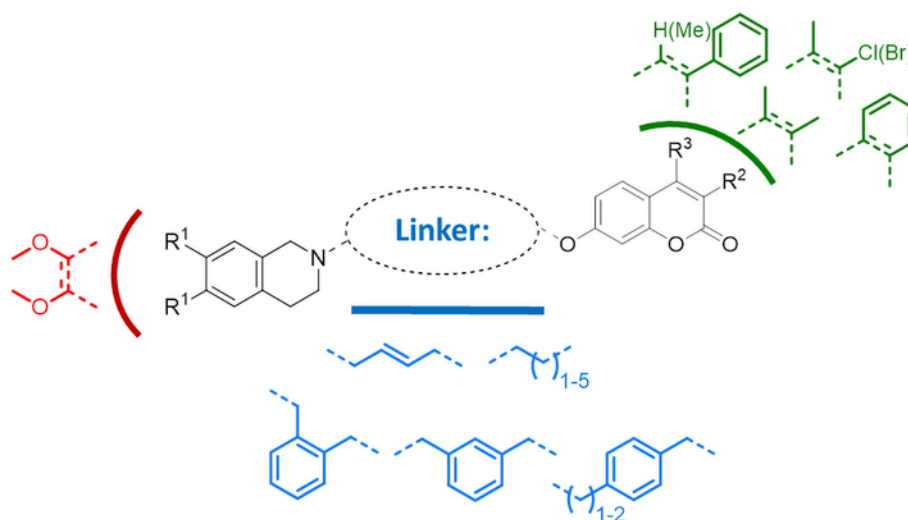


Fig. 1. Rational design of THIQ-coumarin conjugates. Schematic representation of structural modifications addressing the linker and the two heterocyclic scaffolds.

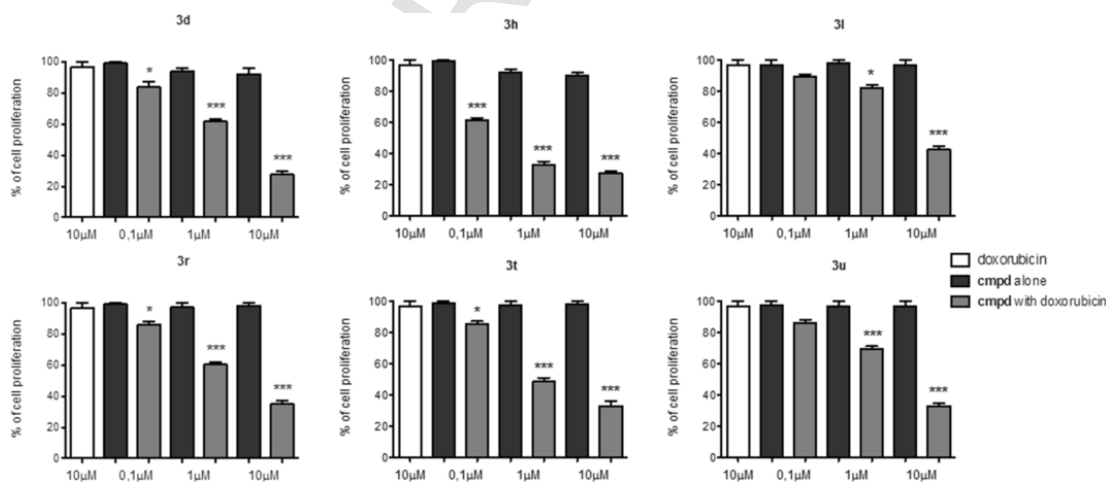
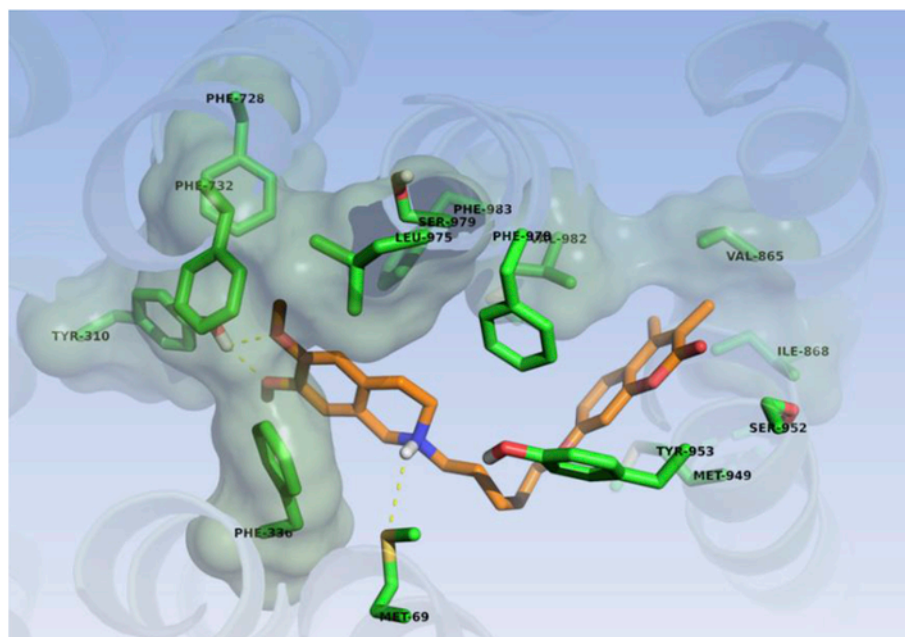


Fig. 2. Dose-dependent effects on in vitro MDCK-MDR1 cells proliferation by compounds **3d**, **3h**, **3l**, **3r**, **3t** and **3u** at three different concentrations (0.1, 1 and  $10\ \mu\text{M}$ ) alone and co-incubated with doxorubicin ( $10\ \mu\text{M}$ ). Cell survival is represented as % of control cell growth in cultures containing no drug and test compounds. Each bar represents the mean  $\pm$  SEM of two experiments in triplicate; one-way ANOVA followed by Bonferroni's post-hoc comparison test: \* $P < 0.1$ , \*\* $P < 0.01$ , \*\*\* $P < 0.001$  vs. doxorubicin alone.



**Fig. 3.** Binding mode of **3h** into the MDR1 binding site. The extracellular and intracellular sides are at top and bottom of the scene, respectively. The free energy of binding calculated with hydration force field of AutoDock is  $-11.93$  kcal/mol, while the contact surface area measures  $411 \text{ \AA}^2$ .

**Table 2**  
Ligand efficiency metrics.

cmpd	clogP <sup>a</sup>	N <sub>HA</sub> <sup>b</sup>	LE <sup>c</sup>	LLE <sup>d</sup>
tariquidar [22]	6.38	47	0.157	0.98
elacridar [32]	7.19	42	0.187	0.66
MC18 [19]	5.36	29	0.204	0.56
<b>3d</b>	5.87	29	0.216	0.39
<b>3h</b>	5.60	33	0.217	1.55
<b>3i</b>	6.17	37	0.182	0.55
<b>3r</b>	5.37	33	0.198	1.18
<b>3t</b>	6.62	37	0.173	-0.21
<b>3u</b>	7.22	38	0.175	-0.56

<sup>a</sup> LogP values calculated with ACD/Labs 6.00.

<sup>b</sup> Number of heavy (non-hydrogen) atoms.

<sup>c</sup> Ligand efficiency (LE) was calculated as  $\text{pIC}_{50}/N_{\text{HA}}$ .

<sup>d</sup> Lipophilic ligand efficiency (LLE) was calculated as  $\text{LLE} = \text{pIC}_{50} - \text{cLogP}$ .

6,7-dimethoxy substituents. The proposed binding mode supported the need of well-defined length and flexibility features of the linker. As a matter of fact, alkyl chain shorter (**3e-g**) or even longer (**3i**) than five carbon units resulted in less active inhibitors. With respect to the coumarin motif, the presence of methyl groups is tolerated and more hindered substituents (**3r**, **3s-u**) cause unfavorable steric clashes with residues of the transmembrane domain, namely Val865, Ile868 and Val982.

#### 4. Conclusion

Herein we described a SAR study on novel derivatives bearing a protonatable THIQ core conjugated through a linker of different length and chemical nature with a differently substituted coumarin motif as inhibitors of P-gp and MRP1 mediated efflux. A systematic exploration addressing the nature of the linker highlighted the pivotal role of length and flexibility in improving P-gp inhibition. Focused structural variations were introduced at coumarin C3-4 region, where steric hindrance proved to be a molecular determinant promoting P-gp selectivity. A number of potent and selective P-gp inhibitors have

been identified and the most potent compound of the series showed nanomolar inhibition potency (**3h**,  $\text{IC}_{50} = 70 \text{ nM}$ ). Docking simulations were employed to gain insight into the binding modes, suggesting the key role of the linker in accommodating the two heterocyclic templates to fit two different lipophilic cages in P-gp in agreement with the observed SARs. Finally, some of these modulators proved able in reverting resistance to doxorubicin and reactivating the cytotoxicity of the antibiotic in MDCK-MDR1 cell lines. These candidates, which showed negligible cytotoxicity, deserve further investigation aimed at developing novel small molecules as therapeutic adjuvants against chemoresistant tumors.

## 5. Experimental section

### 5.1. Chemistry

Starting materials, reagents, and analytical grade solvents were purchased from Sigma-Aldrich (Europe). The purity of all the intermediates, checked by HPLC, was always better than 95%. All the newly prepared and tested compounds showed purity higher than 95% (elemental analysis). Elemental analyses were performed on the EuroEA 3000 analyzer only on the final compounds tested as efflux pumps inhibitors. Analyses indicated by the symbols of the elements were within  $\pm 0.4\%$  of the theoretical values. Column chromatography was performed using Merck silica gel 60 (0.063–0.200 mm, 70–230 mesh). Flash chromatographic separations were performed on a Biotage SP1 purification system using flash cartridges prepacked with KP-Sil 32–63  $\mu\text{m}$ , 60  $\text{\AA}$  silica. All reactions were routinely checked by TLC (thin layer chromatography) using Merck Kieselgel 60  $F_{254}$  aluminum plates and visualized by UV light or iodine. Regarding the reaction requiring the use of dry solvents, the glassware was flame-dried and then cooled under a stream of dry argon before the use. Microwave reactions were performed in a Milestone MicroSynth apparatus, setting temperature and reaction times, fixing maximum irradiation power to 600 W and heating ramp times to 2 min. Nuclear magnetic resonance spectra were recorded on a Varian Mercury 300 instrument (at 300 MHz) or on an Agilent Technologies 500 apparatus



(at 500 MHz) at ambient temperature in the specified deuterated solvent. Chemical shifts ( $\delta$ ) are quoted in parts per million (ppm) and are referenced to the residual solvent peak. The coupling constants  $J$  are given in Hertz (Hz). The following abbreviations were used: s (singlet), d (doublet), dd (doublet of doublet), t (triplet), q (quadruplet), qn (quintuplet), m (multiplet), br s (broad signal); signals due to OH and NH protons were located by deuterium exchange with D<sub>2</sub>O. HRMS experiments were performed with a dual electrospray interface (ESI) and a quadrupole time-of-flight mass spectrometer (Q-TOF, Agilent 6530 Series Accurate-Mass Quadrupole Time-of-Flight LC/MS, Agilent Technologies Italia S.p.A., Cernusco sul Naviglio, Italy). Full-scan mass spectra were recorded in the mass/charge ( $m/z$ ) range 50–3000 Da. Melting points were determined by the capillary method on a Stuart Scientific SMP3 electrothermal apparatus and are uncorrected. 7-Hydroxy-2H-chromen-2-one (**1b**) and 3-chloro-7-hydroxy-4-methyl-2H-chromen-2-one (**1d**) were commercially available. The synthesis of the following intermediates has been already described in the literature: 7-hydroxy-3,4-dimethyl-2H-chromen-2-one [**14**] (**1a**), 7-hydroxy-3-phenyl-2H-chromen-2-one [**17**] (**1e**).

#### 5.1.1. 3-Bromo-7-hydroxy-4-methyl-2H-chromen-2-one (**1c**)

*N*-bromosuccinimide (0.98 g, 5.5 mmol) was added slowly to a suspension of 7-hydroxy-4-methyl-2H-chromen-2-one [**15**] (0.88 g, 5.0 mmol) in PEG-400 (10 g). After stirring at room temperature for 3 h, the reaction mixture was diluted with brine (100 mL) and extracted with CH<sub>2</sub>Cl<sub>2</sub> (3 × 80 mL). The collected organic phases were dried over Na<sub>2</sub>SO<sub>4</sub> and concentrated under reduced pressure. The resulting crude was purified through column chromatography (gradient eluent: ethyl acetate in *n*-hexane 5% → 30%). Pale yellow solid; yield: 0.45 g, 35%. Spectroscopic data are in agreement with those reported in the literature [**16**].

#### 5.1.2. 7-Hydroxy-4-methyl-3-phenyl-2H-chromen-2-one (**1f**)

By applying slight modifications to a previously reported method [**18**], 2',4'-dihydroxyacetophenone (0.76 g, 5.0 mmol) was dissolved in anhydrous acetone (40 mL), before the addition of potassium carbonate (4.1 g, 30 mmol) and phenylacetylchloride (2.0 mL, 15 mmol). The reaction was refluxed for 4 h and then cooled to room temperature. The inorganic residue was filtered-off and the solution was concentrated under rotary evaporation. The crude dark brown solid residue was then purified through column chromatography (gradient eluent: methanol in dichloromethane 0% → 2%). Off white solid; yield: 0.77 g, 61%. <sup>1</sup>H NMR (300 MHz, DMSO-*d*<sub>6</sub>)  $\delta$ : 2.19 (s, 3H), 6.73 (d,  $J=2.2$  Hz, 1H), 6.82 (dd,  $J=8.7, 2.2$  Hz, 1H), 7.21–7.31 (m, 2H), 7.31–7.49 (m, 3H), 7.65 (d,  $J=8.7$  Hz, 1H), 10.49 (s, 1H, dis. with D<sub>2</sub>O).

#### 5.1.3. 3-Hydroxy-6H-benzo[*c*]chromen-6-one (**1g**)

Anhydrous AlCl<sub>3</sub> (2.1 g, 16 mmol) was added to a suspension of 3-methoxy-6H-benzo[*c*]chromen-6-one [**15**] (0.90 g, 4.0 mmol) in *o*-xylene (20 mL) and the reaction mixture was refluxed for 9 h. After cooling to room temperature, the solvent was removed under rotary evaporation. The residue was diluted with CH<sub>2</sub>Cl<sub>2</sub> (200 mL) and washed with 1 N aq. HCl (3 × 40 mL). The organic phase was washed with brine (100 mL) and dried over Na<sub>2</sub>SO<sub>4</sub>. The evaporation of the solvent under reduced pressure yielded a pink solid (0.76 g, 89%) that was used without further purification. Spectroscopic data are in agreement with those reported in the literature [**15**].

#### 5.1.4. General procedure for the synthesis of intermediates **1h**, **2a-g**, **2i-r**

The appropriate 7-hydroxycoumarin **1a-g** (2.0 mmol for **2a-g** and **2i-r**; 3.0 mmol for **1h**) was suspended in anhydrous acetone (10 mL) before adding potassium carbonate (for **2a-g** and **2i-r**: 0.83 g,

6.0 mmol; for **1h**: 1.2 g, 9.0 mmol), the suitable mono-halide (for **1h**: 2-[4-(bromomethyl)phenyl]ethanol, 3.0 mmol) or di-halide (for **2a-g** and **2i-r**: 6.0 mmol of  $\alpha,\alpha'$ -dibromo(chloro)-xylenes or *trans*-1,4-dibromo-2-butene; 10 mmol of 1, $\omega$ -dibromoalkanes) and a catalytic amount of KI in a Pyrex vessel charged with a magnetic stirring bar and a Weflon bar. The vessel was placed in a microwave apparatus and irradiated at 130 °C for 30 min. After cooling to room temperature, the inorganic residue was filtered off after thorough washing with CH<sub>2</sub>Cl<sub>2</sub>. The solution was concentrated to dryness and the resulting crude was purified as detailed below.

#### 5.1.4.1. 7-[4-(2-Hydroxyethyl)benzyl]oxy]-3,4-dimethyl-2H-chromen-2-one (**1h**)

Prepared from **1a** (0.57 g, 3.0 mmol) and 2-[4-(bromomethyl)phenyl]ethanol [**23**] (0.65 g, 3.0 mmol). Purification procedure: the crude solid was washed several times with diethyl ether and the remaining residue was filtered off. The resulting mother liquor was concentrated to dryness, thus yielding the desired product as a white solid (0.92 g, 95%). <sup>1</sup>H NMR (300 MHz, DMSO-*d*<sub>6</sub>)  $\delta$ : 2.03 (s, 3H), 2.33 (s, 3H), 2.70 (t,  $J=7.0$  Hz, 2H), 3.58 (d,  $J=7.0$  Hz, 2H), 4.61 (d,  $J=7.0$  Hz, 1H, dis. with D<sub>2</sub>O), 5.14 (s, 2H), 6.93–7.04 (m, 2H), 7.22 (d,  $J=8.0$  Hz, 2H), 7.35 (d,  $J=8.0$  Hz, 2H), 7.66 (d,  $J=8.7$  Hz, 1H).

#### 5.1.4.2. 7-(2-Bromoethoxy)-3,4-dimethyl-2H-chromen-2-one (**2a**)

Prepared from **1a** (0.38 g, 2.0 mmol) and 1,2-dibromoethane (0.86 mL, 10 mmol). Purification procedure: column chromatography (gradient eluent: ethyl acetate in *n*-hexane 0% → 50%). White solid; yield: 0.17 g, 28%. <sup>1</sup>H NMR (500 MHz, DMSO-*d*<sub>6</sub>)  $\delta$ : 2.06 (s, 3H), 2.35 (s, 3H), 3.82 (t,  $J=7.0$  Hz, 2H), 4.41 (t,  $J=7.0$  Hz, 2H), 6.94–7.00 (m, 2H), 7.70 (d,  $J=8.5$  Hz, 1H).

#### 5.1.4.3. 7-(3-Bromopropoxy)-3,4-dimethyl-2H-chromen-2-one (**2b**)

[**14**] Prepared from **1a** (0.38 g, 2.0 mmol) and 1,3-dibromopropane (1.0 mL, 10 mmol). Purification procedure: flash chromatography (gradient eluent: ethyl acetate in *n*-hexane 0% → 60%). White solid; yield: 0.49 g, 79%. <sup>1</sup>H NMR (500 MHz, DMSO-*d*<sub>6</sub>)  $\delta$ : 2.07 (s, 3H), 2.27 (q,  $J=6.4$  Hz, 2H), 2.36 (s, 3H), 3.67 (t,  $J=6.4$  Hz, 2H), 4.18 (t,  $J=6.4$  Hz, 2H), 6.95–6.98 (m, 2H), 7.70 (d,  $J=8.8$  Hz, 1H).

#### 5.1.4.4. 7-(4-Bromobutoxy)-3,4-dimethyl-2H-chromen-2-one (**2c**)

[**14**] Prepared from **1a** (0.38 g, 2.0 mmol) and 1,4-dibromobutane (1.2 mL, 10 mmol). Purification procedure: flash chromatography (gradient eluent: ethyl acetate in *n*-hexane 0% → 50%). White solid; yield: 0.57 g, 88%. <sup>1</sup>H NMR (500 MHz, DMSO-*d*<sub>6</sub>)  $\delta$ : 1.85 (qn,  $J=6.4$  Hz, 2H), 1.97 (qn,  $J=6.4$  Hz, 2H), 2.07 (s, 3H), 2.36 (s, 3H), 3.61 (t,  $J=6.4$  Hz, 2H), 4.10 (t,  $J=6.4$  Hz, 2H), 6.92–6.95 (m, 2H), 7.68 (d,  $J=8.8$  Hz, 1H).

#### 5.1.4.5. 7-[5-(Bromopentyl)oxy]-3,4-dimethyl-2H-chromen-2-one (**2d**)

Prepared from **1a** (0.38 g, 2.0 mmol) and 1,5-dibromopentane (1.4 mL, 10 mmol). Purification procedure: column chromatography (eluent: ethyl acetate in *n*-hexane 10%). White solid; yield: 0.52 g, 76%. <sup>1</sup>H NMR (500 MHz, CDCl<sub>3</sub>)  $\delta$ : 1.56–1.72 (m, 2H), 1.76–1.89 (m, 2H), 1.89–2.03 (m, 2H), 2.18 (s, 3H), 2.37 (s, 3H), 3.45 (d,  $J=6.3$  Hz, 2H), 4.02 (t,  $J=6.3$  Hz, 2H), 6.78 (d,  $J=2.4$  Hz, 1H), 6.84 (dd,  $J=8.8, 2.4$  Hz, 1H), 7.49 (d,  $J=8.8$  Hz, 1H).

#### 5.1.4.6. 7-[(6-Bromohexyl)oxy]-3,4-dimethyl-2H-chromen-2-one (**2e**)

Prepared from **1a** (0.38 g, 2.0 mmol) and 1,6-dibromohexane (1.5 mL, 10 mmol). Purification procedure: column chromatography (gradient eluent: ethyl acetate in *n*-hexane 10% → 30%). White solid;

yield: 0.28 g, 39%. <sup>1</sup>H NMR (500 MHz, DMSO-*d*<sub>6</sub>) δ: 1.36–1.50 (m, 4H), 1.67–1.75 (m, 2H), 1.78–1.85 (m, 2H), 2.05 (s, 3H), 2.34 (s, 3H), 3.52 (t, *J*=6.7 Hz, 2H), 4.04 (t, *J*=6.7 Hz, 2H), 6.88–6.94 (m, 2H), 7.66 (d, *J*=9.6 Hz, 1H).

#### 5.1.4.7. 7-[(2*E*)-4-Bromobut-2-en-1-yl]oxy}-3,4-dimethyl-2H-chromen-2-one (2f)

Prepared from **1a** (0.38 g, 2.0 mmol) and *trans*-1,4-dibromo-2-butene (1.3 g, 6.0 mmol). Purification procedure: column chromatography (gradient eluent: ethyl acetate in *n*-hexane 10% → 30%). Off-white solid; yield: 0.45 g, 69%. <sup>1</sup>H NMR (500 MHz, DMSO-*d*<sub>6</sub>) δ: 2.06 (s, 3H), 2.39 (s, 3H), 4.18 (d, *J*=6.0 Hz, 2H), 4.69 (d, *J*=3.7 Hz, 2H), 5.92–6.14 (m, 2H), 6.90–6.99 (m, 2H), 7.69 (d, *J*=8.5 Hz, 1H).

#### 5.1.4.8. 7-{[4-(Bromomethyl)benzyl]oxy}-3,4-dimethyl-2H-chromen-2-one (2g)

Prepared from **1a** (0.38 g, 2.0 mmol) and α,α'-dibromo-*p*-xylene (1.6 g, 6.0 mmol). Purification procedure: column chromatography (gradient eluent: ethyl acetate in *n*-hexane 10% → 60%). Off white solid; yield: 0.60 g, 80%. <sup>1</sup>H NMR (300 MHz, DMSO-*d*<sub>6</sub>) δ: 2.05 (s, 3H), 2.35 (s, 3H), 4.70 (s, 2H), 5.20 (s, 2H), 6.96–7.04 (m, 2H), 7.40–7.49 (m, 4H), 7.69 (d, *J*=8.5 Hz, 1H).

#### 5.1.4.9. 7-{[3-(Chloromethyl)benzyl]oxy}-3,4-dimethyl-2H-chromen-2-one (2i)

Prepared from **1a** (0.38 g, 2.0 mmol) and α,α'-dichloro-*m*-xylene (1.1 g, 6.0 mmol). Purification procedure: column chromatography (gradient eluent: ethyl acetate in *n*-hexane 10% → 30%). White solid; yield: 0.62 g, 94%. <sup>1</sup>H NMR (300 MHz, DMSO-*d*<sub>6</sub>) δ: 2.06 (s, 3H), 2.35 (s, 3H), 4.77 (s, 2H), 5.20 (s, 2H), 7.01 (dd, *J*=8.7, 2.5 Hz, 1H), 7.03 (d, *J*=2.5 Hz, 1H), 7.37–7.45 (m, 3H), 7.53 (s, 1H), 7.69 (d, *J*=8.7 Hz, 1H).

#### 5.1.4.10. 7-{[3-(Chloromethyl)benzyl]oxy}-2H-chromen-2-one (2j)

Prepared from **1b** (0.32 g, 2.0 mmol) and α,α'-dichloro-*m*-xylene (1.1 g, 6.0 mmol). Purification procedure: column chromatography (gradient eluent: ethyl acetate in *n*-hexane 10% → 50%). White solid; yield: 0.43 g, 72%. <sup>1</sup>H NMR (500 MHz, DMSO-*d*<sub>6</sub>) δ: 4.78 (s, 2H), 5.22 (s, 2H), 6.28 (d, *J*=9.5 Hz, 1H), 7.02 (dd, *J*=8.6, 2.4 Hz, 1H), 7.08 (d, *J*=2.4 Hz, 1H), 7.36–7.46 (m, 3H), 7.53 (s, 1H), 7.63 (d, *J*=8.6 Hz, 1H), 7.98 (d, *J*=9.5 Hz, 1H).

#### 5.1.4.11. 7-{[2-(Bromomethyl)benzyl]oxy}-3,4-dimethyl-2H-chromen-2-one (2k)

Prepared from **1a** (0.38 g, 2.0 mmol) and α,α'-dibromo-*o*-xylene (1.6 g, 6.0 mmol). Purification procedure: column chromatography (gradient eluent: ethyl acetate in *n*-hexane 10% → 30%). White solid; yield: 0.73 g, 98%. <sup>1</sup>H NMR (500 MHz, DMSO-*d*<sub>6</sub>) δ: 2.07 (s, 3H), 2.36 (s, 3H), 4.82 (s, 2H), 5.34 (s, 2H), 7.04 (dd, *J*=8.8, 2.5 Hz, 1H), 7.10 (d, *J*=2.5 Hz, 1H), 7.34–7.38 (m, 1H), 7.48–7.52 (m, 1H), 7.52–7.56 (m, 1H), 7.57–7.62 (m, 1H), 7.72 (d, *J*=8.8 Hz, 1H).

#### 5.1.4.12. 7-(4-Bromobutoxy)-3-chloro-4-methyl-2H-chromen-2-one (2l)

Prepared from **1d** (0.42 g, 2.0 mmol) and 1,4-dibromobutane (1.2 mL, 10 mmol). Purification procedure: flash chromatography (gradient eluent: ethyl acetate in *n*-hexane 0% → 30%). White solid; yield: 0.35 g, 51%. <sup>1</sup>H NMR (300 MHz, CDCl<sub>3</sub>) δ: 1.94–2.13 (m, 4H), 2.55 (s, 3H), 3.49 (t, *J*=6.1 Hz, 2H), 4.06 (t, *J*=6.1 Hz, 2H), 6.81 (d, *J*=2.5 Hz, 1H), 6.89 (dd, *J*<sub>1</sub>=2.5 Hz, *J*<sub>2</sub>=8.8 Hz, 1H), 7.52 (d, *J*=8.8 Hz, 1H).

#### 5.1.4.13. 7-[(5-Bromopentyl)oxy]-3-chloro-4-methyl-2H-chromen-2-one (2m)

Prepared from **1d** (0.42 g, 2.0 mmol) and 1,5-dibromopentane (1.4 mL, 10 mmol). Purification procedure: column chromatography (gradient eluent: ethyl acetate in *n*-hexane 10% → 30%). White solid; yield: 0.47 g, 66%. <sup>1</sup>H NMR (300 MHz, CDCl<sub>3</sub>) δ: 1.57–1.73 (m, 2H), 1.79–2.00 (m, 4H), 2.55 (s, 3H), 3.45 (t, *J*=6.7 Hz, 2H), 4.03 (t, *J*=6.3 Hz, 2H), 6.81 (d, *J*=2.5 Hz, 1H), 6.89 (dd, *J*=8.9, 2.5 Hz, 1H), 7.52 (d, *J*=8.9 Hz, 1H).

#### 5.1.4.14. 3-Bromo-7-[(5-bromopentyl)oxy]-4-methyl-2H-chromen-2-one (2n)

Prepared from **1c** (0.51 g, 2.0 mmol) and 1,5-dibromopentane (1.4 mL, 10 mmol). Purification procedure: column chromatography (gradient eluent: ethyl acetate in *n*-hexane 10% → 30%). White solid; yield: 0.50 g, 62%. <sup>1</sup>H NMR (300 MHz, DMSO-*d*<sub>6</sub>) δ: 1.43–1.60 (m, 2H), 1.66–1.80 (m, 2H), 1.80–1.97 (m, 2H), 2.56 (s, 3H), 3.54 (t, *J*=6.6 Hz, 2H), 4.08 (t, *J*=6.3 Hz, 2H), 6.97 (dd, *J*=8.9, 2.3 Hz, 1H), 7.02 (d, *J*=2.3 Hz, 1H), 7.77 (d, *J*=8.9 Hz, 1H).

#### 5.1.4.15. 7-(4-Bromobutoxy)-3-phenyl-2H-chromen-2-one (2o)

Prepared from **1e** (0.48 g, 2.0 mmol) and 1,4-dibromobutane (1.2 mL, 10 mmol). Purification procedure: flash chromatography (gradient eluent: ethyl acetate in *n*-hexane 0% → 30%). White solid; yield: 0.69 g, 92%. <sup>1</sup>H NMR (300 MHz, DMSO-*d*<sub>6</sub>) δ: 1.81–2.06 (m, 4H), 3.60 (t, *J*=6.6 Hz, 2H), 4.12 (t, *J*=6.3 Hz, 2H), 6.97 (dd, *J*<sub>1</sub>=2.2 Hz, *J*<sub>2</sub>=8.8 Hz, 1H), 7.03 (d, *J*=2.2 Hz, 1H), 7.34–7.46 (m, 3H), 7.66–7.70 (m, 3H), 8.19 (s, 1H).

#### 5.1.4.16. 7-[(5-Bromopentyl)oxy]-3-phenyl-2H-chromen-2-one (2p)

Prepared from **1e** (0.48 g, 2.0 mmol) and 1,5-dibromopentane (1.4 mL, 10 mmol). Purification procedure: column chromatography (gradient eluent: ethyl acetate in *n*-hexane 10% → 30%). White solid; yield: 0.62 g, 80%. <sup>1</sup>H NMR (300 MHz, DMSO-*d*<sub>6</sub>) δ: 1.44–1.61 (m, 2H), 1.67–1.93 (m, 4H), 3.55 (t, *J*=6.7 Hz, 2H), 4.09 (t, *J*=6.4 Hz, 2H), 6.96 (dd, *J*=8.6, 2.4 Hz, 1H), 7.02 (d, *J*=2.4 Hz, 1H), 7.33–7.47 (m, 3H), 7.62–7.73 (m, 3H), 8.19 (s, 1H).

#### 5.1.4.17. 7-[(5-Bromopentyl)oxy]-4-methyl-3-phenyl-2H-chromen-2-one (2q)

Prepared from **1f** (0.50 g, 2.0 mmol) and 1,5-dibromopentane (1.4 mL, 10 mmol). Purification procedure: column chromatography (gradient eluent: ethyl acetate in *n*-hexane 10% → 20%). White solid; yield: 0.67 g, 83%. <sup>1</sup>H NMR (300 MHz, DMSO-*d*<sub>6</sub>) δ: 1.47–1.62 (m, 2H), 1.66–1.81 (m, 2H), 1.81–1.97 (m, 2H), 2.22 (s, 3H), 3.56 (t, *J*=6.7 Hz, 2H), 4.10 (t, *J*=6.4 Hz, 2H), 6.93–7.03 (m, 2H), 7.23–7.32 (m, 2H), 7.32–7.49 (m, 3H), 7.74 (d, *J*=8.7 Hz, 1H).

#### 5.1.4.18. 3-[(5-Bromopentyl)oxy]-6H-benzo[*c*]chromen-6-one (2r)

Prepared from **1g** (0.42 g, 2.0 mmol) and 1,5-dibromopentane (1.4 mL, 10 mmol). Purification procedure: column chromatography (eluent: ethyl acetate in *n*-hexane 70%). White solid; yield: 0.30 g, 41%. <sup>1</sup>H NMR (300 MHz, CDCl<sub>3</sub>) δ: 1.57–1.73 (m, 2H), 1.77–2.05 (m, 4H), 3.46 (t, *J*=6.7 Hz, 2H), 4.05 (t, *J*=6.3 Hz, 2H), 6.85 (d, *J*=2.5 Hz, 1H), 6.91 (dd, *J*=8.8, 2.5 Hz, 1H), 7.47–7.56 (m, 1H), 7.74–7.83 (m, 1H), 7.95 (d, *J*=8.8 Hz, 1H), 8.01 (d, *J*=8.0 Hz, 1H), 8.36 (dd, *J*=8.0, 1.3 Hz, 1H).

#### 5.1.5. 7-{[4-(2-Bromoethyl)benzyl]oxy}-3,4-dimethyl-2H-chromen-2-one (2h)

Carbon tetrabromide (0.73 g, 2.2 mmol) was added to a solution of **1h** (0.65 g, 2.0 mmol) in anhydrous dichloromethane (10 mL). The mixture was cooled to 0 °C through an external ice bath and then a



solution of triphenylphosphine (0.63 g, 2.4 mmol) in an. dichloromethane (5 mL) was added dropwise. After warming at room temperature, the reaction was kept under magnetic stirring for 4 h. The mixture was concentrated under vacuum and the crude product was purified through column chromatography (gradient eluent: ethyl acetate in *n*-hexane 20% → 40%). White solid; yield: 0.45 g, 58%. <sup>1</sup>H NMR (300 MHz, DMSO-*d*<sub>6</sub>) δ: 2.05 (s, 3H), 2.34 (s, 3H), 3.11 (t, *J*=7.2 Hz, 2H), 3.71 (t, *J*=7.2 Hz, 2H), 5.16 (s, 2H), 6.94–7.04 (m, 2H), 7.29 (d, *J*=8.0 Hz, 2H), 7.40 (d, *J*=8.0 Hz, 2H), 7.68 (d, *J*=8.7 Hz, 1H).

#### 5.1.6. General procedure for the synthesis of final compounds **3a-v**

The appropriate intermediate **2a-r** (0.50 mmol) was suspended in anhydrous acetonitrile (4 mL) followed by the addition of DIPEA (0.52 mL, 3.0 mmol), the suitable 1,2,3,4-tetrahydroisoquinoline hydrochloride (0.75 mmol) and a catalytic amount of KI. The mixture was refluxed for 1 h. After cooling to room temperature, the solvent was removed under rotary evaporation and the residue was purified through column chromatography as detailed below.

##### 5.1.6.1. 7-[2-(3,4-Dihydroisoquinolin-2(1H)-yl)ethoxy]-3,4-dimethyl-2H-chromen-2-one (**3a**)

Prepared from **2a** (0.15 g, 0.50 mmol) and 1,2,3,4-tetrahydroisoquinoline hydrochloride (0.13 g, 0.75 mmol). Purification procedure: column chromatography (gradient eluent: ethyl acetate in *n*-hexane 0% → 40%). Brown solid; yield: 0.10 g, 59%; mp: 141–3 °C. <sup>1</sup>H NMR (500 MHz, DMSO-*d*<sub>6</sub>) δ: 2.06 (s, 3H), 2.35 (s, 3H), 2.71–2.83 (m, 4H), 2.88 (t, *J*=5.7 Hz, 2H), 3.66 (s, 2H), 4.26 (t, *J*=5.7 Hz, 2H), 6.96 (dd, *J*=8.8, 2.2 Hz, 1H), 6.99 (d, *J*=2.2 Hz, 1H), 7.00–7.04 (m, 1H), 7.05–7.12 (m, 3H), 7.68 (d, *J*=8.8 Hz, 1H). Anal. C<sub>22</sub>H<sub>23</sub>NO<sub>3</sub> (C, H, N). HRMS (Q-TOF) calcd for C<sub>22</sub>H<sub>23</sub>NO<sub>3</sub> [*M*+H]<sup>+</sup> *m/z* 350.1751, found 350.1747; [*M*+Na]<sup>+</sup> *m/z* 372.1570, found 372.1568.

##### 5.1.6.2. 7-[3-(3,4-Dihydroisoquinolin-2(1H)-yl)propoxy]-3,4-dimethyl-2H-chromen-2-one (**3b**)

Prepared from **2b** (0.16 g, 0.50 mmol) and 1,2,3,4-tetrahydroisoquinoline hydrochloride (0.13 g, 0.75 mmol). Purification procedure: column chromatography (gradient eluent: ethyl acetate in *n*-hexane 20% → 70%). Off-white solid; yield: 0.13 g, 74%; mp (**3b**-hydrochloride) [14]: >250 °C. <sup>1</sup>H NMR (300 MHz, DMSO-*d*<sub>6</sub>) δ: 1.98 (qn, *J*=6.4 Hz, 2H), 2.05 (s, 3H), 2.34 (s, 3H), 2.59 (t, *J*=6.4 Hz, 2H), 2.65 (t, *J*=5.8 Hz, 2H), 2.79 (t, *J*=5.8 Hz, 2H), 3.55 (s, 2H), 4.13 (t, *J*=6.4 Hz, 2H), 6.91–6.94 (m, 2H), 7.01–7.09 (m, 4H), 7.66 (d, *J*=9.9 Hz, 1H). Anal. C<sub>23</sub>H<sub>25</sub>NO<sub>3</sub> (C, H, N). HRMS (Q-TOF) calcd for C<sub>23</sub>H<sub>25</sub>NO<sub>3</sub> [*M*+H]<sup>+</sup> *m/z* 364.1907, found 364.1906.

##### 5.1.6.3. 7-[4-(3,4-Dihydroisoquinolin-2(1H)-yl)butoxy]-3,4-dimethyl-2H-chromen-2-one (**3c**)

Prepared from **2c** (0.16 g, 0.50 mmol) and 1,2,3,4-tetrahydroisoquinoline hydrochloride (0.13 g, 0.75 mmol). Purification procedure: column chromatography (gradient eluent: ethyl acetate in *n*-hexane 20% → 70%). White solid; yield: 0.14 g, 72%; mp (**3c**-hydrochloride) [14]: 206–8 °C. <sup>1</sup>H NMR (500 MHz, DMSO-*d*<sub>6</sub>) δ: 1.67 (qn, *J*=6.9 Hz, 2H), 1.79 (qn, *J*=6.9 Hz, 2H), 2.07 (s, 3H), 2.36 (s, 3H), 2.46–2.48 (m, 2H), 2.64 (t, *J*=5.4 Hz, 2H), 2.79 (t, *J*=5.4 Hz, 2H), 3.53 (s, 2H), 4.10 (t, *J*=6.9 Hz, 2H), 6.92–6.96 (m, 2H), 7.01–7.08 (m, 4H), 7.67 (d, *J*=9.8 Hz, 1H). Anal. C<sub>24</sub>H<sub>27</sub>NO<sub>3</sub> (C, H, N). HRMS (Q-TOF) calcd for C<sub>24</sub>H<sub>27</sub>NO<sub>3</sub> [*M*+H]<sup>+</sup> *m/z* 378.2064, found 378.2056; [*M*+Na]<sup>+</sup> *m/z* 400.1883, found 400.1885.

##### 5.1.6.4. 7-[[5-(3,4-Dihydroisoquinolin-2(1H)-yl)pentyl]oxy]-3,4-dimethyl-2H-chromen-2-one (**3d**)

Prepared from **2d** (0.17 g, 0.50 mmol) and 1,2,3,4-tetrahydroisoquinoline hydrochloride (0.13 g, 0.75 mmol). Purification procedure:

column chromatography (gradient eluent: ethyl acetate in *n*-hexane 30% → 60%). Pale yellow solid; yield: 0.12 g, 62%; mp: 66–8 °C. <sup>1</sup>H NMR (300 MHz, DMSO-*d*<sub>6</sub>) δ: 1.38–1.51 (m, 2H), 1.51–1.64 (m, 2H), 1.68–1.84 (m, 2H), 2.05 (s, 3H), 2.34 (s, 3H), 2.38–2.44 (m, 2H), 2.61 (d, *J*=5.6 Hz, 2H), 2.77 (t, *J*=5.6 Hz, 2H), 3.50 (s, 2H), 4.05 (t, *J*=6.4 Hz, 2H), 6.87–6.94 (m, 2H), 7.01 (d, *J*=3.9 Hz, 1H), 7.03–7.12 (m, 3H), 7.66 (d, *J*=9.5 Hz, 1H). Anal. C<sub>25</sub>H<sub>29</sub>NO<sub>3</sub> (C, H, N). HRMS (Q-TOF) calcd for C<sub>25</sub>H<sub>29</sub>NO<sub>3</sub> [*M*+H]<sup>+</sup> *m/z* 392.2220, found 392.2219; [*M*+Na]<sup>+</sup> *m/z* 414.2040, found 414.2038.

##### 5.1.6.5. 7-[2-(6,7-Dimethoxy-3,4-dihydroisoquinolin-2(1H)-yl)ethoxy]-3,4-dimethyl-2H-chromen-2-one (**3e**)

Prepared from **2a** (0.15 g, 0.50 mmol) and 6,7-dimethoxy-1,2,3,4-tetrahydroisoquinoline hydrochloride (0.17 g, 0.75 mmol). Purification procedure: flash column chromatography (gradient eluent: ethyl acetate in *n*-hexane 30% → 80%). Pale yellow solid; yield: 0.16 g, 76%; mp: 107–9 °C (dec.). <sup>1</sup>H NMR (500 MHz, DMSO-*d*<sub>6</sub>) δ: 2.07 (s, 3H), 2.36 (s, 3H), 2.67–2.76 (m, 4H), 2.87 (t, *J*=5.7 Hz, 2H), 3.58 (s, 2H), 3.68 (s, 3H), 3.69 (s, 3H), 4.26 (t, *J*=5.7 Hz, 2H), 6.61 (s, 1H), 6.65 (s, 1H), 6.97 (dd, *J*=8.8, 2.5 Hz, 1H), 7.00 (d, *J*=2.5 Hz, 1H), 7.70 (d, *J*=8.8 Hz, 1H). Anal. C<sub>24</sub>H<sub>27</sub>NO<sub>5</sub> (C, H, N). HRMS (Q-TOF) calcd for C<sub>24</sub>H<sub>27</sub>NO<sub>5</sub> [*M*+H]<sup>+</sup> *m/z* 410.1962, found 410.1962.

##### 5.1.6.6. 7-[3-(6,7-Dimethoxy-3,4-dihydroisoquinolin-2(1H)-yl)propoxy]-3,4-dimethyl-2H-chromen-2-one (**3f**)

Prepared from **2b** (0.16 g, 0.50 mmol) and 6,7-dimethoxy-1,2,3,4-tetrahydroisoquinoline hydrochloride (0.17 g, 0.75 mmol). Purification procedure: flash column chromatography (gradient eluent: ethyl acetate in *n*-hexane 30% → 80%). Orange solid; yield: 0.14 g, 68%; mp: 84–6 °C. <sup>1</sup>H NMR (500 MHz, DMSO-*d*<sub>6</sub>) δ: 1.96–2.02 (m, 2H), 2.07 (s, 3H), 2.36 (s, 3H), 2.58 (t, *J*=7.0 Hz, 2H), 2.62 (7, *J*=5.7 Hz, 2H), 2.71 (d, *J*=5.7 Hz, 2H), 3.47 (s, 2H), 3.68 (s, 3H), 3.69 (s, 3H), 4.14 (t, *J*=6.3 Hz, 2H), 6.62 (s, 1H), 6.64 (s, 1H), 6.91–6.97 (m, 2H), 7.68 (d, *J*=9.5 Hz, 1H). Anal. C<sub>25</sub>H<sub>29</sub>NO<sub>5</sub> (C, H, N). HRMS (Q-TOF) calcd for C<sub>25</sub>H<sub>29</sub>NO<sub>5</sub> [*M*+H]<sup>+</sup> *m/z* 424.2118, found 424.2110; [*M*+Na]<sup>+</sup> *m/z* 446.1938, found 446.1935.

##### 5.1.6.7. 7-[4-(6,7-Dimethoxy-3,4-dihydroisoquinolin-2(1H)-yl)butoxy]-3,4-dimethyl-2H-chromen-2-one (**3g**)

Prepared from **2c** (0.16 g, 0.50 mmol) and 6,7-dimethoxy-1,2,3,4-tetrahydroisoquinoline hydrochloride (0.17 g, 0.75 mmol). Purification procedure: flash column chromatography (gradient eluent: ethyl acetate in *n*-hexane 30% → 80%). Off white solid; yield: 0.17 g, 79%; mp: 122–4 °C. <sup>1</sup>H NMR (500 MHz, DMSO-*d*<sub>6</sub>) δ: 1.67 (qn, *J*=6.8 Hz, 2H), 1.78 (qn, *J*=6.8 Hz, 2H), 2.07 (s, 3H), 2.35 (s, 3H), 2.47 (t, *J*=6.8 Hz, 2H), 2.60 (d, *J*=5.6 Hz, 2H), 2.69 (t, *J*=5.6 Hz, 2H), 3.44 (s, 2H), 3.67 (s, 3H), 3.68 (s, 3H), 4.10 (t, *J*=6.8 Hz, 2H), 6.60 (s, 1H), 6.63 (s, 1H), 6.91–6.96 (m, 2H), 7.66 (d, *J*=9.6 Hz, 1H). Anal. C<sub>26</sub>H<sub>31</sub>NO<sub>5</sub> (C, H, N). HRMS (Q-TOF) calcd for C<sub>26</sub>H<sub>31</sub>NO<sub>5</sub> [*M*+H]<sup>+</sup> *m/z* 438.2275, found 438.2274; [*M*+Na]<sup>+</sup> *m/z* 460.2094, found 460.2098.

##### 5.1.6.8. 7-[[5-(6,7-Dimethoxy-3,4-dihydroisoquinolin-2(1H)-yl)pentyl]oxy]-3,4-dimethyl-2H-chromen-2-one (**3h**)

Prepared from **2d** (0.17 g, 0.50 mmol) and 6,7-dimethoxy-1,2,3,4-tetrahydroisoquinoline hydrochloride (0.17 g, 0.75 mmol). Purification procedure: column chromatography (eluent: methanol in dichloromethane 10%). Pale yellow solid; yield: 0.072 g, 32%; mp: 112–4 °C (dec.). <sup>1</sup>H NMR (300 MHz, DMSO-*d*<sub>6</sub>) δ: 1.37–1.47 (m, 2H), 1.50–1.60 (m, 2H), 1.69–1.80 (m, 2H), 2.05 (s, 3H), 2.31 (s, 3H), 2.36–2.44 (m, 2H), 2.52–2.61 (m, 2H), 2.61–2.76 (m, 2H), 3.41 (s, 2H), 3.66 (s, 3H), 3.67 (s, 3H), 4.05 (t, *J*=6.4 Hz, 2H), 6.59 (s, 1H), 6.62 (s, 1H), 6.86–6.99 (m, 2H), 7.66 (d, *J*=9.4 Hz, 1H). Anal. C<sub>27</sub>H<sub>33</sub>NO<sub>5</sub> (C, H, N). HRMS (Q-TOF) calcd for C<sub>27</sub>H<sub>33</sub>NO<sub>5</sub> [*M*+H]<sup>+</sup>



4H), 6.56 (s, 1H), 6.62 (s, 1H), 6.78 (d,  $J=2.4$  Hz, 1H), 6.89 (dd,  $J=8.9, 2.4$  Hz, 1H), 7.51 (d,  $J=8.9$  Hz, 1H). Anal.  $C_{26}H_{30}ClNO_5$  (C, H, N). HRMS (Q-TOF) calcd for  $C_{26}H_{30}ClNO_5$   $[M+H]^+$   $m/z$  472.1885, found 472.1857;  $[M+Na]^+$   $m/z$  494.1705, found 494.1702.

#### 5.1.6.18. 3-Bromo-7- $\{[5-(6,7\text{-dimethoxy-3,4-dihydroisoquinolin-2(1H-yl)pentyl]oxy\}$ -4-methyl-2H-chromen-2-one (3r)

Prepared from **2n** (0.20 g, 0.50 mmol) and 6,7-dimethoxy-1,2,3,4-tetrahydroisoquinoline hydrochloride (0.17 g, 0.75 mmol). Purification procedure: column chromatography (gradient eluent: methanol in dichloromethane 0%  $\rightarrow$  2%). Pale yellow solid; yield: 0.088 g, 34%; mp: 71–3 °C (dec.).  $^1H$  NMR (300 MHz,  $CDCl_3$ )  $\delta$ : 1.44–1.72 (m, 2H), 1.77–2.00 (m, 4H), 2.59 (s, 3H), 2.74–2.92 (m, 2H), 2.97–3.15 (m, 2H), 3.75–3.89 (m, 8H), 3.89–4.11 (m, 4H), 6.53 (s, 1H), 6.62 (s, 1H), 6.80 (d,  $J=2.4$  Hz, 1H), 6.88 (dd,  $J=8.9, 2.4$  Hz, 1H), 7.55 (d,  $J=8.9$  Hz, 1H). Anal.  $C_{26}H_{30}BrNO_5$  (C, H, N). HRMS (Q-TOF) calcd for  $C_{26}H_{30}BrNO_5$   $[M+Na]^+$   $m/z$  538.1200, found 538.1201.

#### 5.1.6.19. 7- $\{[4-(6,7\text{-Dimethoxy-3,4-dihydroisoquinolin-2(1H-yl)butoxy\}$ -3-phenyl-2H-chromen-2-one (3s)

Prepared from **2o** (0.19 g, 0.50 mmol) and 6,7-dimethoxy-1,2,3,4-tetrahydroisoquinoline hydrochloride (0.17 g, 0.75 mmol). Purification procedure: column chromatography (gradient eluent: methanol in dichloromethane 0%  $\rightarrow$  2%). Yellow solid; yield: 0.11 g, 47%; mp: 132–4 °C.  $^1H$  NMR (300 MHz,  $CDCl_3$ )  $\delta$ : 1.73–1.97 (m, 4H), 2.60 (t,  $J=7.1$  Hz, 2H), 2.74 (t,  $J=5.7$  Hz, 2H), 2.84 (t,  $J=5.7$  Hz, 2H), 3.58 (s, 2H), 3.82 (s, 3H), 3.83 (s, 3H), 4.08 (t,  $J=6.2$  Hz, 2H), 6.52 (s, 1H), 6.59 (s, 1H), 6.81–6.88 (m, 2H), 7.33–7.48 (m, 4H), 7.63–7.72 (m, 2H), 7.75 (s, 1H). Anal.  $C_{30}H_{31}NO_5$  (C, H, N). HRMS (Q-TOF) calcd for  $C_{30}H_{31}NO_5$   $[M+H]^+$   $m/z$  486.2275, found 486.2264;  $[M+Na]^+$   $m/z$  508.2094, found 508.2096.

#### 5.1.6.20. 7- $\{[5-(6,7\text{-Dimethoxy-3,4-dihydroisoquinolin-2(1H-yl)pentyl]oxy\}$ -3-phenyl-2H-chromen-2-one (3t)

Prepared from **2p** (0.19 g, 0.50 mmol) and 6,7-dimethoxy-1,2,3,4-tetrahydroisoquinoline hydrochloride (0.17 g, 0.75 mmol). Purification procedure: column chromatography (gradient eluent: methanol in dichloromethane 1%  $\rightarrow$  2%). Pale yellow solid; yield: 0.17 g, 70%; mp: 128–130 °C (dec.).  $^1H$  NMR (300 MHz,  $DMSO-d_6$ )  $\delta$ : 1.38–1.58 (m, 2H), 1.66–1.92 (m, 4H), 2.79–3.10 (m, 2H), 3.10–3.35 (m, 4H), 3.53–3.79 (m, 8H), 4.11 (t,  $J=6.2$  Hz, 2H), 6.76 (s, 1H), 6.80 (s, 1H), 6.96 (dd,  $J=8.6, 2.3$  Hz, 1H), 7.01 (d,  $J=2.3$  Hz, 1H), 7.32–7.49 (m, 3H), 7.61–7.72 (m, 3H), 8.18 (s, 1H). Anal.  $C_{31}H_{33}NO_5$  (C, H, N). HRMS (Q-TOF) calcd for  $C_{31}H_{33}NO_5$   $[M+H]^+$   $m/z$  500.2431, found 500.2429;  $[M+Na]^+$   $m/z$  522.2251, found 522.2255.

#### 5.1.6.21. 7- $\{[5-(6,7\text{-Dimethoxy-3,4-dihydroisoquinolin-2(1H-yl)pentyl]oxy\}$ -4-methyl-3-phenyl-2H-chromen-2-one (3u)

Prepared from **2q** (0.20 g, 0.50 mmol) and 6,7-dimethoxy-1,2,3,4-tetrahydroisoquinoline hydrochloride (0.17 g, 0.75 mmol). Purification procedure: column chromatography (gradient eluent: methanol in dichloromethane 0%  $\rightarrow$  2%). Yellow solid; yield: 0.11 g, 44%; mp: 168–170 °C (dec.).  $^1H$  NMR (300 MHz,  $CDCl_3$ )  $\delta$ : 1.50–1.67 (m, 2H), 1.75–1.99 (m, 4H), 2.27 (s, 3H), 2.67–2.86 (m, 2H), 2.91–3.08 (m, 4H), 3.72–3.93 (m, 8H), 4.06 (t,  $J=6.2$  Hz, 2H), 6.54 (s, 1H), 6.61 (s, 1H), 6.83 (d,  $J=2.4$  Hz, 1H), 6.88 (dd,  $J=8.8, 2.4$  Hz, 1H), 7.25–7.32 (m, 2H), 7.33–7.51 (m, 3H), 7.56 (d,  $J=8.8$  Hz, 1H). Anal.  $C_{32}H_{35}NO_5$  (C, H, N). HRMS (Q-TOF) calcd for  $C_{32}H_{35}NO_5$   $[M+H]^+$   $m/z$  514.2588, found 514.2586;  $[M+Na]^+$   $m/z$  536.2407, found 536.2409.

#### 5.1.6.22. 3- $\{[5-(6,7\text{-Dimethoxy-3,4-dihydroisoquinolin-2(1H-yl)pentyl]oxy\}$ -6H-benzo[*c*]chromen-6-one (3v)

Prepared from **2r** (0.18 g, 0.50 mmol) and 6,7-dimethoxy-1,2,3,4-tetrahydroisoquinoline hydrochloride (0.17 g, 0.75 mmol). Purification procedure: column chromatography (eluent: methanol in dichloromethane 5%). Yellow solid; yield: 0.11 g, 45%; mp: 106–8 °C (dec.).  $^1H$  NMR (300 MHz,  $CDCl_3$ )  $\delta$ : 1.64–1.49 (m, 2H), 1.65–1.79 (m, 2H), 1.82–1.96 (m, 2H), 2.53–2.71 (m,  $J=8.7$  Hz, 2H), 2.75–2.94 (m, 4H), 3.67 (s, 2H), 3.83 (s, 3H), 3.84 (s, 3H), 4.04 (t,  $J=6.4$  Hz, 2H), 6.52 (s, 1H), 6.59 (s, 1H), 6.85 (d,  $J=2.5$  Hz, 1H), 6.90 (dd,  $J=8.8, 2.5$  Hz, 1H), 7.45–7.55 (m, 1H), 7.73–7.83 (m, 1H), 7.89–8.03 (m, 2H), 8.36 (d,  $J=8.0$  Hz, 1H). Anal.  $C_{29}H_{31}NO_5$  (C, H, N). HRMS (Q-TOF) calcd for  $C_{29}H_{31}NO_5$   $[M+H]^+$   $m/z$  474.2275, found 474.2267;  $[M+Na]^+$   $m/z$  496.2094, found 496.2090.

## 5.2. Biological assays

### 5.2.1. Materials

CulturePlate 96/wells plates were purchased from PerkinElmer Life and Analytical Sciences (Boston, MA, USA). Calcein-AM, doxorubicin and MTT (3-[4,5-dimethylthiazol-2-yl]-2,5-diphenyltetrazoliumbromide) were purchased from Sigma-Aldrich-RBI s.r.l. (Milan, Italy). Cell culture medium and reagents were purchased from EuroClone (Milan, Italy) and Sigma-Aldrich.

### 5.2.2. Cell cultures

MDCK-MDR1 and MDCK-MRP1 are a gift of Prof. P. Borst, NKI-AVL Institute, Amsterdam, Netherlands. MDCK-MDR1, MDCK-MRP1 were grown in DMEM high glucose supplemented with 10% fetal bovine serum (FBS), 2 mM glutamine, 100 U/mL penicillin, 100  $\mu$ g/mL streptomycin, in a humidified incubator at 37 °C with a 5%  $CO_2$  atmosphere.

### 5.2.3. Calcein-AM assays

According to a previously reported procedure [24], MDCK-MDR1 or MDCK-MRP1 cell lines (50,000 cells per well) were seeded into black CulturePlate 96/wells plate with 100  $\mu$ L medium and grown overnight to confluence. Aliquots (100  $\mu$ L) of tested compounds in culture medium, at scalar concentrations ranging from 0.1 to 100  $\mu$ M, were added to each well. The plate was incubated at 37 °C for 30 min. Calcein-AM in phosphate buffered saline (PBS, 100  $\mu$ L) was added to each well at a final concentration of 2.5  $\mu$ M, and the plate was incubated for 30 min. The plate was washed 3 times with 100 mL ice cold PBS. Saline buffer (100  $\mu$ L) was added to each well and the plate was read by a PerkinElmer Victor3 spectrofluorimeter at excitation and emission wavelengths of 485 nm and 535 nm, respectively. Under these conditions, calcein cell accumulation in the absence and in the presence of tested compounds was evaluated, and a fluorescence basal level was estimated by untreated cells. In treated wells, the increase of fluorescence with respect to the basal level was measured.  $IC_{50}$  values were determined by fitting the fluorescence increase percentage versus  $\log[\text{dose}]$  with GraphPad Prism Software 5.0 (GraphPad Software, Inc.: San Diego, CA).

### 5.2.4. Antiproliferative assay

The co-administration assay with doxorubicin was performed in MDCK-MDR1 cells at 72 h [25]. On day 1, 10,000 cells/well were seeded into 96-well plates in a volume of 100  $\mu$ L. On day 2, the compounds under study, each in three concentrations (0.1, 1, and 10  $\mu$ M), were added. On day 3, the medium was removed and the tested compounds, each in three concentrations, were added alone and in combination with 10  $\mu$ M doxorubicin. In all the experiments, the solvents (EtOH, DMSO) were added in each control to evaluate their cytotoxicity.

city. After the established incubation time, 0.5 mg/mL MTT was added to each well and after 3 h incubation at 37 °C the supernatant was removed. The formazan crystals were solubilized using 100  $\mu$ L of DMSO and the absorbance values at 570 and 630 nm were determined on the microplate reader Victor 3. Data were analyzed by one-way ANOVA (GraphPad Prism 5.0) for repeated measures followed by post-hoc Bonferroni's multiple comparison test. Results are expressed as mean  $\pm$  SD of at 2–3 independent experiments in triplicates. Statistical significance was accepted at a level of  $P < 0.05$ .

### 5.3. Molecular docking studies

The molecular model of the ligand **3h** in protonated form, with standard values of bond lengths and valence angles, was built within Maestro software package [26], while Marsili-Gasteiger charges were calculated with the molcharge suite of QUACPAC [27]. The THIQ dihedral ring angles were tailored according to the puckering observed in the previously reported X-ray of the structurally related P-gp inhibitor MC70 [28]. AMBER FF14SB force field charges were assigned to MDR1 protein structure within CHIMERA 1.11 [29]. Due to the flexibility of the ligand and a large extension of the binding surface, in order to assess a reliable bioactive conformation molecular dynamics sampling followed by docking to MDR1 structure were carried out according to similar studies performed on the same biomolecular target [21]. In detail, the **3h** solvated structure was assembled using the Desmond system builder tool implemented in Maestro [30], and stochastic molecular dynamics were performed using the default settings and relaxation protocol of Desmond on a NVIDIA Quadro M4000 GPU at constant temperature (300 K) and pressure (1 bar) for a total of 500 ns, storing energies and trajectory frames each 250 ps. An initial screening of the sampled 2000 conformations was first carried out with VINA 1.1.2 [31] submitting each structures to rigid body dockings, increasing the search space size by 30 Å in each of the three dimension from the center of its binding site comprising residues Met69, Tyr310, Phe336, Phe728, Ala729, Phe732, Met949, Ser952, Tyr953, Leu975, Phe978, Ser979, Val982, Phe983, Met986. Afterwards the refinement of VINA poses was obtained as follows: affinity maps were calculated on a 65  $\times$  65  $\times$  65 cubic box 0.375 Å spaced, and a local optimization with AUTODOCK 4.2.6 [32] was used in a ligand-receptor flexible docking to estimate the free energy of binding (FEB) as scoring function. The best FEB solution was then selected as representative of the binding mode of compound **3h**.

### Author contributions

L.P. designed and supervised the project, contributed to the synthesis, made the literature research and wrote the paper. M.R. carried out the synthesis and the physico-chemical characterization. M.N. carried out the in vitro screening and revised the paper. A.C. performed the docking studies and contributed to write the paper. N.A.C. analyzed and supervised the in vitro screening. S.C. supervised the synthesis and revised the manuscript. C.D.A. supervised the project and contributed to write the paper. All authors have given approval to the final version of the manuscript.

### Acknowledgements

This work was supported by University of Bari "Aldo Moro". L.P. acknowledges financial support from APQ Research Apulian Region "FutureInResearch (FKY7YJ5) - Regional program for smart specialization and social and environmental sustainability" Fondo di Sviluppato e Coesione 2007–2013.

### Appendix A. Supplementary data

Supplementary data to this article can be found online at <https://doi.org/10.1016/j.ejmech.2018.10.043>.

### References

- [1] G. Szakács, J.K. Paterson, J.A. Ludwig, C. Booth-Genthe, M.M. Gottesman, Targeting multidrug resistance in cancer, *Nat. Rev. Drug Discov.* 5 (2006) 219–234.
- [2] G. Housman, S. Byler, S. Heerboth, K. Lapinska, M. Longacre, N. Snyder, S. Sarkar, Drug resistance in cancer: an overview, *Cancers* 6 (2014) 1769–1792.
- [3] M.M. Gottesman, T. Fojo, S.E. Bates, Multidrug resistance in cancer: role of ATP-dependent transporters, *Nat. Rev. Canc.* 2 (2002) 48–58.
- [4] M. Dean, A. Rzhetsky, R. Allikmets, The human ATP binding cassette (ABC) transporter superfamily, *Genome Res.* 11 (2001) 1156–1166.
- [5] N.A. Colabufo, F. Berardi, M. Cantore, M. Contino, C. Inglese, M. Niso, R. Perrone, Perspectives of P-glycoprotein modulating agents in oncology and neurodegenerative diseases: pharmaceutical, biological, and diagnostic potentials, *J. Med. Chem.* 53 (2010) 1883–1897.
- [6] S.P.C. Cole, Multidrug resistance protein 1 (MRP1, ABCC1), a "multitasking" ATP-binding cassette (ABC) transporter, *J. Biol. Chem.* 289 (2014) 30880–30888.
- [7] D. Waghray, Q. Zhang, Inhibit or evade multidrug resistance P-glycoprotein in cancer treatment, *J. Med. Chem.* 61 (2018) 5108–5121.
- [8] R.W. Robey, K.M. Pluchino, M.D. Hall, A.T. Fojo, S.E. Bates, M.M. Gottesman, Revisiting the role of ABC transporters in multidrug-resistant cancer, *Nat. Rev. Canc.* 18 (2018) 452–464.
- [9] A.H. Abuznait, A. Kaddoumi, Role of ABC transporters in the pathogenesis of Alzheimer's disease, *ACS Chem. Neurosci.* 3 (2012) 820–831.
- [10] S. Emami, S. Dadashpour, Current developments of coumarin-based anti-cancer agents in medicinal chemistry, *Eur. J. Med. Chem.* 102 (2015) 611–630.
- [11] L. Pisani, R. Farina, R. Soto-Otero, N. Denora, G.F. Mangiatordi, O. Nicolotti, E. Mendez-Alvarez, C.D. Altomare, M. Catto, A. Carotti, Searching for multi-targeting neurotherapeutics against Alzheimer's: discovery of potent AChE-MAO B inhibitors through the decoration of the 2H-chromen-2-one structural motif, *Molecules* 21 (2016) 362–376.
- [12] L. Pisani, R. Farina, O. Nicolotti, D. Gadaleta, R. Soto-Otero, M. Catto, M. Di Braccio, E. Mendez-Alvarez, A. Carotti, In silico design of novel 2H-chromen-2-one derivatives as potent and selective MAO-B inhibitors, *Eur. J. Med. Chem.* 89 (2015) 98–105.
- [13] A.R. Quesada, M.D. García Grávalos, J.L. Fernández Puentes, Polyaromatic alkaloids from marine invertebrates as cytotoxic compounds and inhibitors of multidrug resistance caused by P-glycoprotein, *Br. J. Canc.* 74 (1996) 677–682.
- [14] L. Pisani, R. Farina, M. Catto, R.M. Iacobazzi, O. Nicolotti, S. Cellamare, G.F. Mangiatordi, N. Denora, R. Soto-Otero, L. Siragusa, C.D. Altomare, A. Carotti, Exploring basic tail modifications of coumarin-based dual acetylcholinesterase-monoamine oxidase B inhibitors: identification of water-soluble, brain-permeant neuroprotective multitarget agents, *J. Med. Chem.* 59 (2016) 6791–6806.
- [15] L. Pisani, M. Catto, I. Giangreco, F. Leonetti, O. Nicolotti, A. Stefanachi, S. Cellamare, A. Carotti, Design, synthesis and biological evaluation of coumarin derivatives tethered to an edrophonium-like fragment as highly potent and selective dual binding site acetylcholinesterase inhibitors, *ChemMedChem* 5 (2010) 1616–1630.
- [16] K. Venkateswarlu, K. Suneel, B. Das, K.N. Reddy, T.S. Reddy, Simple catalyst-free regio- and chemoselective monobromination of aromatics using NBS in polyethylene glycol, *Synth. Commun.* 39 (2008) 215–219.
- [17] A. Fais, M. Corda, B. Era, M.B. Fadda, M.J. Matos, E. Quezada, L. Santana, C. Picciau, G. Podda, G. Delogu, Tyrosinase inhibitor activity of coumarin-resveratrol hybrids, *Molecules* 14 (2009) 2514–2520.
- [18] L. Xie, Y. Takeuchi, L.M. Cosentino, A.T. McPhail, K.H. Lee, Anti-AIDS agents. 42. Synthesis and anti-HIV activity of disubstituted (3'R,4'R)-3',4'-di-O-(S)-camphanoyl-(+)-cis-khellactone analogues, *J. Med. Chem.* 44 (2001) 664–671.
- [19] N.A. Colabufo, F. Berardi, M. Cantore, M.G. Perrone, M. Contino, C. Inglese, M. Niso, R. Perrone, A. Azzariti, L. Porcelli, G.M. Simone, A. Paradiso, Small P-gp modulating molecules: SAR studies on tetrahydroisoquinoline derivatives, *Bioorg. Med. Chem.* 16 (2008) 362–373.
- [20] F. Denizot, R. Lang, Rapid colorimetric assay for cell growth and survival. modifications to the tetrazolium dye procedure giving improved sensitivity and reliability, *J. Immunol. Methods* 89 (1986) 271–277.
- [21] S. Guglielmo, L. Lazzarato, M. Contino, M.G. Perrone, K. Chegaev, A. Carrieri, R. Fruttero, N.A. Colabufo, A. Gasco, Structure-activity relationship studies on tetrahydroisoquinoline derivatives: [4'-(6,7-dimethoxy-3,4-dihydro-1H-isouquinolin-2-ylmethyl)biphenyl-4-ol] (MC70) conjugated through flexible alkyl chains

- with furazan moieties gives rise to potent and selective ligands of P-glycoprotein, *J. Med. Chem.* 59 (2016) 6729–6738.
- [22] E. Teodori, S. Dei, G. Bartolucci, M.G. Perrone, D. Manetti, M.N. Romanelli, M. Contino, N.A. Colabufo, Structure–activity relationship studies on 6,7-dimethoxy-2-phenethyl-1,2,3,4-tetrahydroisoquinoline derivatives as multidrug resistance reversers, *ChemMedChem* 12 (2017) 1369–1379.
- [23] R. Farina, L. Pisani, M. Catto, O. Nicolotti, D. Gadaleta, N. Denora, R. Soto-Otero, E. Mendez-Alvarez, C.S. Passos, G. Muncipinto, C.D. Altomare, A. Nurisio, P.A. Carrupt, A. Carotti, Structure-based design and optimization of multitarget-directed 2H-chromen-2-one derivatives as potent inhibitors of monoamine oxidase B and cholinesterases, *J. Med. Chem.* 58 (2015) 5561–5578.
- [24] M. Niso, M.L. Pati, F. Berardi, C. Abate, Rigid versus flexible anilines or anilides confirm the bicyclic ring as the hydrophobic portion for optimal  $\sigma_2$  receptor binding and provide novel tools for the development of future  $\sigma_2$  receptor PET radiotracers, *RSC Adv.* 6 (2016) 88508–88518.
- [25] A.A. Nevskaya, M.D. Matveeva, T.N. Borisova, M. Niso, N.A. Colabufo, A. Boccarelli, R. Purgatorio, M. de Candia, S. Cellamare, L.G. Voskressensky, C.D. Altomare, A new class of 1-aryl-5,6-dihydropyrrolo[2,1-a]isoquinoline derivatives as reversers of P-glycoprotein-mediated multidrug resistance in tumor cells, *ChemMedChem* (2018) <https://doi.org/10.1002/cmdc.201800177>.
- [26] Schrödinger Release 2018-1, Maestro, Schrödinger, LLC, New York, NY, 2017.
- [27] QUACPAC 1.7.0.2: OpenEye Scientific Software, Santa Fe, NM. <http://www.eyesopen.com>.
- [28] A. Altomare, E. Capparelli, A. Carrieri, N.A. Colabufo, A. Moliterni, R. Rizzi, D. Siliqi, Crystallographic study of PET radio-tracers in clinical evaluation for early diagnosis of Alzheimers, *Acta Crystallogr. E* 70 (2014) 1149–1150.
- [29] E.F. Pettersen, T.D. Goddard, C.C. Huang, G.S. Couch, D.M. Greenblatt, E.C. Meng, T.E. Ferrin, UCSF Chimera--a visualization system for exploratory research and analysis, *J. Comput. Chem.* 25 (2004) 1605–1612.
- [30] K.J. Bowers, E. Chow, H. Xu, R.O. Dror, M.P. Eastwood, B.A. Gregersen, J.L. Klepeis, I. Kolossvary, M.A. Moraes, F.D. Sacerdoti, J.K. Salmon, Y. Shan, D.E. Shaw, Scalable algorithms for molecular dynamics simulations on commodity clusters, In: Proceedings of the ACM/IEEE Conference on Supercomputing (SC06), Tampa, Florida, 2006, November 11-17 Schrödinger Release 2015-3: Desmond Molecular Dynamics System, Version 4.3, D. E. Shaw Research, New York, NY, 2015, Maestro-Desmond Interoperability Tools, version 4.3, Schrödinger, New York, NY, 2015.
- [31] O. Trott, A.J. Olson, AutoDock Vina, Improving the speed and accuracy of docking with a new scoring function, efficient optimization and multithreading, *J. Comput. Chem.* 31 (2010) 455–461.
- [32] G.M. Morris, D.S. Goodsell, R.S. Halliday, R. Huey, W.E. Hart, R.K. Belew, A.J. Olson, Automated Docking using a Lamarckian genetic algorithm and empirical binding free energy function, *J. Comput. Chem.* 19 (1998) 1639–1662.